Nigerian Journal of Physics (NJP)
ISSN online: 3027-0936
ISSN print: 1595-0611
DOI: https://doi.org/10.62292/njp.v35(s).2026.693
Volume 35(S), 2026

Integrated Geoelectrical and Geospatial Assessment of Groundwater Variation in Selected Location over Port Harcourt, Rivers State, Nigeria

[1]Usamat Sulyman, [1]Godwin Babatunde Egbeyale,
[1]Adegbenro Sunday Ajani and [2]Salami A. Oladipupo

[1]Kwara State University, Malete
[2]Federal College of Fisheries and Marine Technology, Victoria Island, Lagos

*Corresponding Author's Email: usamatsulyman8@gmail.com

Keywords:
Groundwater Potential,
Aquifer Vulnerability,
Vertical Electrical Sounding,
Geographic Information System,
Analytic Hierarchy Process,
Port Harcourt

Submitted: 07 Aug. 2026

Accepted: 31 Aug. 2026

Published: 11 Sept. 2026

ABSTRACT

Groundwater is the major source of potable water in Port Harcourt, Rivers State, Nigeria, owing to increasing degradation of surface water resources resulting from rapid urbanization, industrialization, and population growth. This study integrates Vertical Electrical Sounding (VES), Geographic Information Systems (GIS), Remote Sensing (RS), and the Analytic Hierarchy Process (AHP) to evaluate groundwater potential and aquifer vulnerability in the study area. Ten VES stations were investigated using the Schlumberger electrode configuration with current electrode spacing ranging from 2 to 200 m. The interpreted geoelectrical parameters were used to estimate aquifer hydraulic properties, including hydraulic conductivity, transmissivity, longitudinal conductance, transverse resistance, porosity, and permeability. Four groundwater conditioning factors, rainfall, geology, lineament density, and soil type, were integrated within a GIS environment using AHP to generate the Groundwater Potential Index (GWPI). The AHP weighting identified rainfall (55.8%) as the dominant groundwater conditioning factor, followed by geology (26.3%), lineament density (12.2%), and soil type (5.7%), with a consistency ratio of 0.045, indicating reliable pairwise judgments. Hydraulic conductivity ranged from 0.0839 to 28.7584 m/day, transmissivity from 6.1 to 853.1 m²/day, porosity from 0.1764 to 0.6870, and permeability from 100.32 to 34,380 mD, demonstrating considerable spatial heterogeneity in aquifer properties. The GWPI map classified the study area into Very Low, Low, Moderate, High, and Very High groundwater potential zones, with the western, northwestern, and central sectors exhibiting the most favourable groundwater conditions. Validation against VES-derived transmissivity showed 100% agreement, comprising 50% excellent and 50% good correspondence between the GIS-AHP predictions and geoelectrical interpretations. The integrated approach provides a reliable framework for groundwater exploration, borehole siting, aquifer protection, and sustainable groundwater resources management in rapidly urbanizing coastal environments.

INTRODUCTION

Groundwater is the largest readily accessible freshwater resource and supplies drinking water to nearly half of the global population (UNESCO, 2022). Increasing population growth, urbanization, industrialization, and climate change have intensified dependence on groundwater, particularly in developing countries where public water supply is inadequate (Taylor *et al.*, 2013). However, anthropogenic activities such as industrial discharge, oil exploration, agriculture, urban expansion, and poor waste management have significantly increased groundwater vulnerability to contamination, threatening water security and public health (Foster & Chilton, 2003; Wakode *et al.*, 2018).

Groundwater occurrence and movement are governed by geological formations, lithology, structural features, topography, and climatic conditions. Conventional methods such as drilling and pumping tests provide reliable hydrogeological information but are costly, time-consuming, and spatially limited (Doro *et al.*, 2020). In contrast, electrical resistivity techniques, particularly Vertical Electrical Sounding (VES), provide rapid and cost-effective characterization of subsurface lithology and estimation of key aquifer hydraulic parameters, including hydraulic conductivity, transmissivity, permeability, and porosity (Adeniji *et al*., 2013; George *et al*., 2017; Singh & Singh, 2016). These parameters are fundamental for groundwater exploration and sustainable aquifer management.

Recent advances in Geographic Information Systems (GIS), Remote Sensing (RS), and Multi-Criteria Decision-Making (MCDM) techniques have improved groundwater investigations through the integration of multiple hydrogeological controlling factors (Aladeboyeje *et al*., 2021). The Analytic Hierarchy Process (AHP) developed by Saaty (1980) is widely applied to assign relative weights to groundwater conditioning factors and delineate groundwater potential and vulnerability zones (Jasmin & Mallikarjuna, 2014; Preeja *et al*., 2011). However, many studies rely solely on either geophysical or geospatial approaches, limiting assessment reliability because surface-based predictions are often not validated using field-derived subsurface data.

Port Harcourt, located within the eastern Niger Delta Basin, is a rapidly urbanizing metropolitan area where groundwater serves as the primary source of potable water due to widespread degradation of surface water resources (Ogbozige & Toko, 2020). Rapid urban growth, proliferation of shallow boreholes, inadequate sanitation, industrial activities, and oil-related pollution have increased the risk of groundwater contamination and raised concerns regarding aquifer sustainability (George *et al*., 2014). Despite the importance of groundwater in the area, integrated studies combining geoelectrical investigations with GIS-based groundwater potential and vulnerability assessment remain limited.

This study integrates Vertical Electrical Sounding (VES), geoelectrical-derived hydraulic parameters, Remote Sensing, GIS, and the Analytic Hierarchy Process (AHP) to evaluate groundwater potential and vulnerability in Port Harcourt, Rivers State, Nigeria. By combining subsurface geophysical data with spatial environmental information, the study characterizes aquifer properties, delineates groundwater potential zones, evaluates aquifer protective capacity, and validates geospatial predictions using field-derived geoelectrical data. The findings provide a scientific basis for groundwater exploration, borehole siting, aquifer protection, urban planning, and sustainable water resources management in rapidly urbanizing coastal environments.

Geology and Hydrogeology of the Study Area

Rivers State, located within the Niger Delta complex, is distinguished by fine-to-coarse sand layers typical of fluvial channel deposits. The region's geology is separated into two main formations: the Quaternary Deltaic Plain (upper and lower units) and the Tertiary Benin and Ameki Formations (Tamunobereton-ari *et al*., 2014). The Deltaic Plain is made up mostly of coarse-to-medium grained, unconsolidated sands organized in lenticular beds, interspersed with layers of peaty material, soft silt, clay, and shale. The sandy layers of this formation act as very productive aquifers. The high permeability of the Benin formation, the overlaying lateritic red earth and worn top of the formation, as well as the underlying clay-shale member of the Bende-Ameki and Ogwashi-Asaba formation, offer the hydrologic conditions that favour aquifer development in the area (Short & Stauble, 1967; Kogbe, 1989). Groundwater is encountered in two distinct aquifer systems referred to as the Shallow Groundwater and Deep Superficial Aquifer. Depending on the season, the shallow groundwater is found 6–8 meters below the ground surface, just beneath the superficial clays. It is anticipated that the hydraulic link between the shallow system and the groundwater discharge into the deeper aquifer would exist. Water tables or potentiometric surface levels of the saturated zone in Rivers State, particularly in all the centres selected for the case study, range from 5 to 10 meters for shallow aquifers and from 15 to 35 meters for deep aquifers with a high recharge capacity because of the weather patterns, the amount, and the time window of precipitation in a year, according to the Rivers State Ministry of Water Resources (Tamunobereton-ari *et al*., 2013; Tamunobereton-ari *et al*., 2014).

The Benin formation, which comprises the auriferous zone of interest in the study area, is mainly sandy (>90%) with a few intercalations of shale beds; the sands and sandstones are coarse-grained and mainly colored by feldspar minerals, limonite coating, and hematite grains; the shales are silty or greyish-brown, and they contain scattered lignite and plant remains. These landforms are frequently obscured by dense vegetation, which includes mangrove swamps near the coast and secondary to freshwater marsh flora in the interior region. The majority of pollutants or contaminants that are deposited on the ground surface and those that are drained inside this layer and occluded to the fine particles of the clay material and the organic materials of the vegetative cover are absorbed by the top clayey thick vegetative vegetation layer (Alloway & Ayres, 1997; Tamunobereton-ari *et al*., 2014). The unconsolidated sands of the Benin Formation consist of freshwater-bearing sands characterized by high porosity (Todd & Mays, 2005; Short & Stauble, 1967; Telford *et al*., 1990). The site is in the mangrove freshwater marsh hydrogeological province, which is primarily made up of deltaic plains. Aquifers can be located in different places and at varying depths, and their water quality varies.

MATERIALS AND METHODS

Study Location

The study area is Port Harcourt, Rivers State, located in southern Nigeria. It lies approximately between longitudes 6°55′ E and 7°10′ E and latitudes 4°45′ N and 4°55′ N (figure 1). Port Harcourt is the capital city of Rivers State and one of Nigeria's most densely populated urban centers. It is a major commercial, industrial, and administrative hub, renowned as the heart of the country's oil and gas industry (Adegbola *et al*., 2023). The city hosts the headquarters and operational facilities of several international oil companies (IOCs), as well as numerous petroleum-related industries. In addition to hydrocarbon exploration and production, the local economy is supported by commerce, manufacturing, transportation, and service industries. Rapid urbanization, high population density, extensive road networks, and increasing industrial activities have contributed to growing environmental pressures, making groundwater quality and protection important concerns for sustainable water resource management..

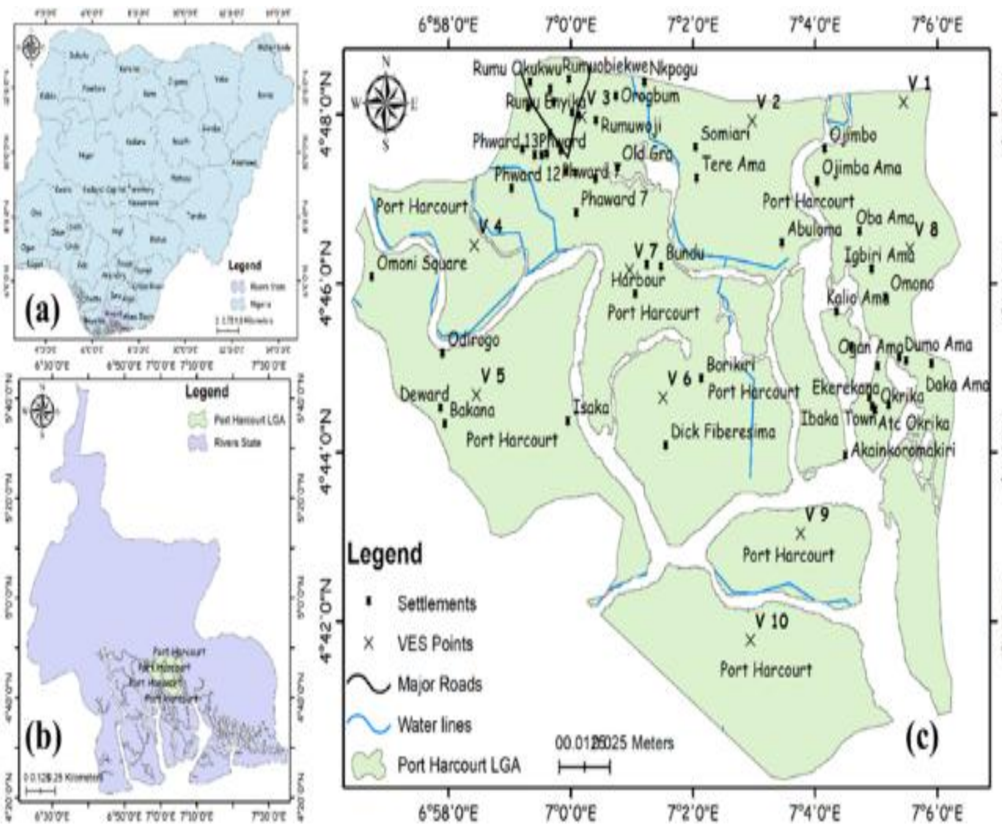

Figure 1: Schematic Map of (a) Nigeria, Showing Rivers State, (b)Map of Rivers State, Showing Port Harcourt and (c) Map of Port Harcourt Highlighting the Study Area Where the Survey was Conducted

Materials

The resources used for this study include resistivity meter and other accessories, software such as IPI2Win for VES modeling and ArcGIS for map contouring. The ABEM Terrameter SAS 300 B resistivity meter, along with its accessories, was employed in the fieldwork. The meter operates on an internal 12-volt, 75-amp battery, which supplies external power through an integrated connection (ABEM Instrument, 2010). SAS is an abbreviation for Signal Averaging System, a technique that automates sequential measurements and constantly averages the findings (Gemail *et al*., 2011). It was chosen above other systems because its findings are more consistent than those obtained from single-shot methods. The sounding locations' precise geographical coordinates and elevations were obtained using a portable global positioning system (GPS) receiver.

1-D Resistivity Data Acquisition and Processing

A one-dimensional Vertical Electrical Sounding (VES) survey was conducted at ten (10) locations across Port Harcourt, Rivers State, Nigeria, using an ABEM Terrameter SAS 300B and the Schlumberger electrode configuration. In this array, electric current was introduced into the subsurface through the outer current electrodes (A and B), while the resulting potential difference was measured between the inner potential electrodes (M and N). The measured resistance values were subsequently used to compute the apparent resistivity of the subsurface.

The Schlumberger configuration was selected because it provides a relatively large depth of investigation with fewer electrode movements, making it suitable for groundwater exploration and aquifer characterization (Salami *et al*., 2024). During field measurements, the current electrode spacing (AB) was progressively increased from 2 to 200 m, while the potential electrode spacing (MN) varied from 0.5 to 20 m, increasing only when the measured potential difference became too small for accurate recording. Throughout the survey, careful attention was given to maintaining proper electrode alignment, minimizing contact resistance, and ensuring good electrode-to-ground contact to improve data quality (Obinawu *et al*., 2011).

The apparent resistivity (ρ_a) was calculated from the measured resistance (Ra) using the Schlumberger geometric factor according to Equation (1):

$$\rho_a = \pi \cdot \left[\frac{(AB/2)^2 - (MN/2)^2}{MN} \right] \cdot R_a \qquad (1)$$

where AB stands for current electrode separation and MN for potential electrode separation.

The calculated apparent resistivity values were plotted on logarithmic scales using Microsoft Excel to assess data quality and identify anomalous measurements before inversion. The processed data were subsequently interpreted using IPI2Win (Version 3.0), a one-dimensional inversion software package (Bobachev, 2002). Initial models were constrained using available borehole lithological information to improve the reliability of the inversion results. The inversion produced the principal geoelectrical parameters, including layer resistivity, thickness, and depth, with acceptable model convergence achieved at root mean square (RMS) errors generally below 5%.

Figure 2, 3 and 4 presents the interpreted sounding curves for VES 1–VES 10, including the observed field data and the corresponding theoretical inversion models. The close agreement between the measured and calculated apparent resistivity responses indicates satisfactory model convergence and confirms the reliability of the derived geoelectrical parameters. These results provide a robust basis for the subsequent estimation of aquifer hydraulic properties and groundwater potential assessment (Uwa *et al*., 2018).

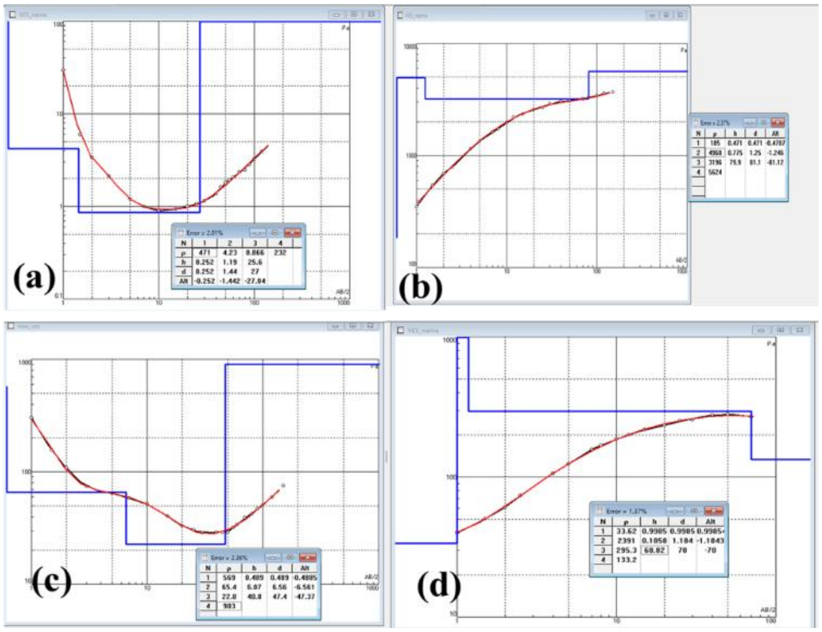

Figure 2: Interpreted VES Sounding Curves for VES 1–4: (a) VES 1, (b) VES 2, (c) VES 3, and (d) VES 4

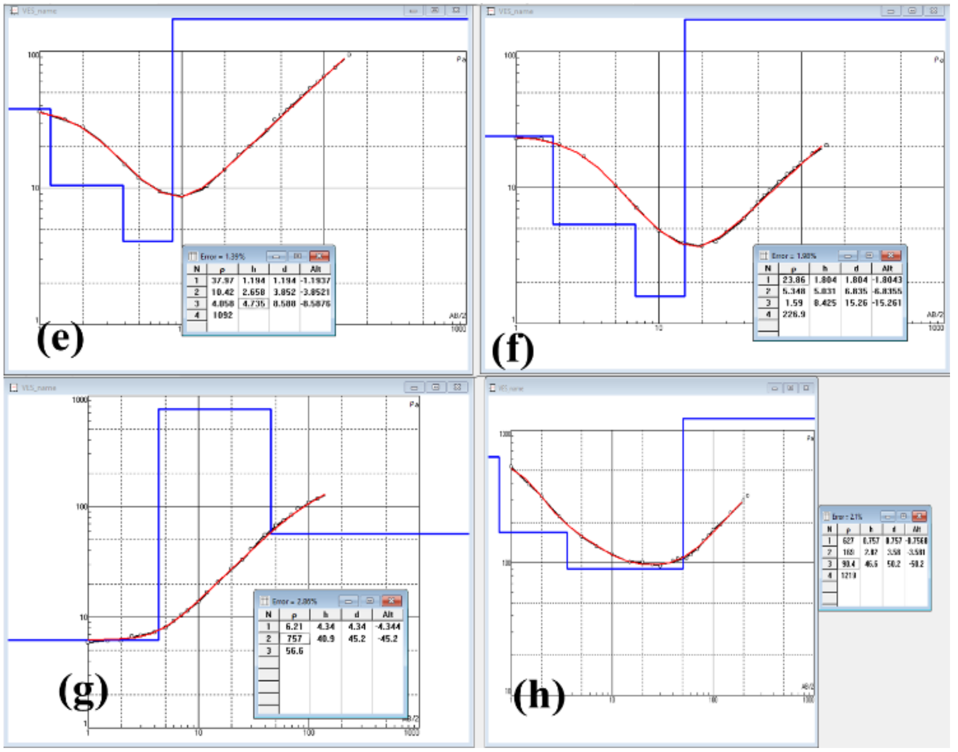

Figure 3: Interpreted VES Sounding Curves for VES 5–8: (e) VES 5, (f) VES 6, (g) VES 7, and (h) VES 8

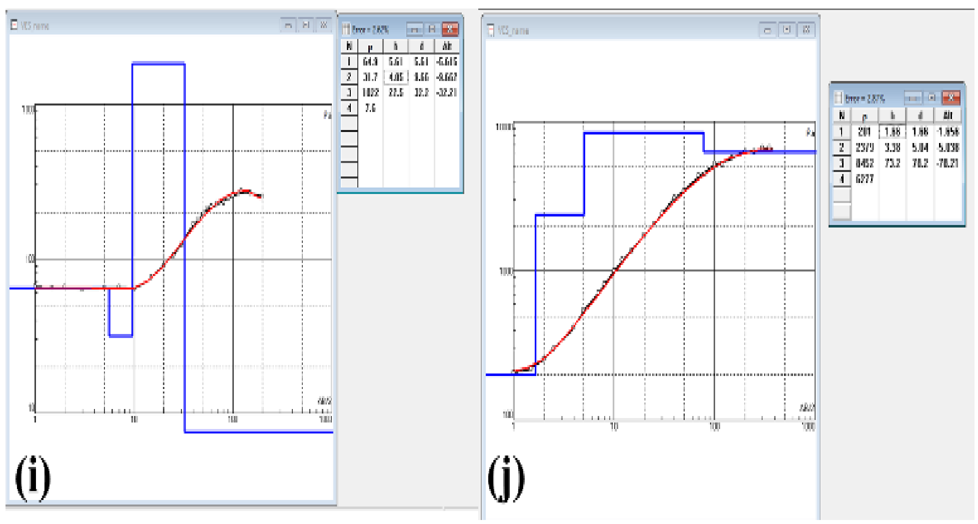

Figure 4: Interpreted VES Sounding Curves for VES 9–10: (i) VES 9 and (j) VES 10

RESULTS AND DISCUSSION

Vertical Electrical Sounding Interpretation and Hydrogeoelectric Characteristics

The interpreted Vertical Electrical Sounding (VES) results for the ten (10) survey locations are summarized in Table 1. The interpretation was performed using manual curve matching and computer-assisted inversion, resulting in excellent agreement between the observed and calculated apparent resistivity curves. The inversion models yielded root mean square (RMS) errors ranging from 1.08% to 2.86%, all below the generally accepted threshold of 5%, confirming the reliability of the interpreted geoelectrical models.

Table 1: Summary of VES results in the Study Locations from VES 1 to 50

VES No	Long (Degrees)	Lat (degrees)	Layer Resistivity Ωm)						Layer thickness (m)				Depth (m)				RMS Error
			Elev (m)	ρ_1	ρ_2	ρ_3	ρ_4	P_5	h_1	h_2	h3	h4	d_1	d_2	d_3	d4	
VES 1	4.75043	7.00772	17.00	1609.00	66.90	16.20	25.30	5986.00	0.35	1.30	10.70	26.6	0.35	1.65	12.35	38.95	2.22
VES 2	4.75068	7.00844	27.00	185.00	4960.00	3196.00	5624.00	---	0.47	0.78	79.90	---	0.47	1.25	81.15	---	2.37
VES 3	4.79858	6.97599	5.00	569.00	65.40	22.80	903.00	---	0.49	6.07	40.80	---	0.49	6.56	47.36	---	2.29
VES 4	4.78715	6.97956	2.27	33.62	2391.00	295.30	133.20	---	1.00	0.19	68.82	---	1.00	1.18	70.00	---	1.37
VES 5	4.76667	7.01718	60.00	382.30	112.30	47.97	710.80	---	0.35	1.09	41.41	---	0.35	1.44	42.85	---	1.21
VES 6	4.82405	7.00811	23.00	639.00	102.90	49.78	8969.00	---	0.47	1.70	49.74	---	0.47	2.17	51.91	---	1.08
VES 7	4.76629	7.00990	12.00	6.21	757.00	56.60		---	4.34	40.90		---	4.34	45.24		---	2.86
VES 8	4.76146	7.02375	38.00	627.00	169.00	90.40	1219.00	---	0.76	2.82	46.60	---	0.76	3.58	50.18	---	2.10
VES 9	4.79732	7.06259	14.00	64.90	31.70	1822.00	7.60	---	5.61	4.05	22.50	---	5.61	9.66	32.16	---	2.64
VES 10	4.75625	7.03598	20.00	201.00	2379.00	8452.00	6277.00	---	1.66	3.38	73.20	---	1.66	5.04	78.24	---	2.37

The interpreted subsurface generally consists of four geoelectric layers, although VES 1 exhibits a five-layer model and VES 7 a three-layer model, reflecting lateral variations in lithology across the study area. The first-layer resistivity varies from 6.21 Ωm at VES 7 to 1,609 Ωm at VES 1, with thicknesses ranging from 0.35 to 5.61 m, indicating considerable variability in the near-surface materials. The second-layer resistivity ranges between 31.7 and 4,960 Ωm, with thicknesses varying from 0.19 to 40.90 m, suggesting significant lateral changes within the weathered zone and shallow aquifer materials. The third layer exhibits resistivity values between 16.2 and 8,452 Ωm and thicknesses of 10.70–79.90 m, representing the principal aquifer horizon and underlying formations. Where present, the fourth-layer resistivity ranges from 7.6 to 8,969 Ωm, while the fifth layer, identified only at VES 1, records a resistivity of 5,986 Ωm. The close correspondence between the measured and calculated sounding curves confirms the reliability of the interpreted layer resistivities and thicknesses used for subsequent hydrogeological analyses (Ekanem *et al*., 2025).

The interpreted geoelectrical parameters were further used to estimate the hydrogeoelectric characteristics of the aquifer system (Table 2), including transverse resistance, longitudinal conductance, hydraulic conductivity, transmissivity, water conductivity, water resistivity, bulk resistivity, saturated formation resistivity, formation factor, unsaturated-zone resistivity, porosity, and permeability. These parameters provide quantitative information on aquifer productivity, groundwater storage, groundwater flow, and aquifer protective capacity. The estimated transverse resistance ranges from 173.30 to 618,686.40 Ωm², with a mean value of 97,410.42 Ωm², indicating substantial variation in aquifer thickness and electrical properties. Longitudinal conductance varies from 0.0183 to 1.8831 mhos, suggesting spatial differences in the protective capacity of the overburden, where higher values generally correspond to thicker clay-rich layers capable of attenuating contaminant migration. Hydraulic conductivity ranges from 0.0839 to 28.7584 m/day, while transmissivity varies from 6.10 to 853.10 m²/day, demonstrating pronounced variability in groundwater flow capacity and aquifer productivity across the study area. Areas characterized by relatively high hydraulic conductivity and transmissivity are expected to possess greater groundwater yield potential than areas with lower values. Bulk resistivity ranges from 16.20 to 8,452.00 Ωm, whereas saturated formation resistivity varies from 1.62 to 7,950.68 Ωm, reflecting differences in lithology, clay content, groundwater saturation, and pore-water quality. Water resistivity ranges from 14.60 to 501.30 Ωm, while water conductivity varies between 0.0020 and 0.0686 S/m, indicating variations in dissolved ionic concentration within the groundwater. The estimated formation factor ranges from 1.11 to 16.86, while total porosity varies from 0.1764 to 0.6870, reflecting differences in pore geometry, grain Packing and interconnected pore spaces. Permeability ranges from 100.32 to 34,380 mD, indicating substantial spatial variability in the ease with which groundwater can flow through the aquifer matrix. In general, locations exhibiting relatively high porosity, permeability, hydraulic conductivity, and transmissivity are interpreted to possess favourable groundwater potential (Todd & Mays, 2005; Alaminiokuma & Warmate, 2020). The VES interpretation and derived hydrogeoelectric parameters reveal a heterogeneous shallow aquifer system controlled by variations in lithology, grain size distribution, sediment packing, degree of sorting, and interconnected pore spaces within the Benin Formation. Similar hydrogeoelectric heterogeneity and spatial variations in aquifer hydraulic properties have been reported for Port Harcourt and other parts of the Niger Delta, where alternating sands, clayey sands, and clay layers strongly influence groundwater occurrence, storage, and flow characteristics (Eke & Life-George, 2018; Alaminiokuma & Warmate, 2020; Ogbozige & Toko, 2020) lithology, degree of weathering, grain-size distribution, clay content, and groundwater saturation. The observed spatial variability demonstrates that groundwater occurrence and productivity differ considerably across Port Harcourt. The derived hydrogeoelectric parameters therefore provide a reliable basis for delineating groundwater potential zones, evaluating aquifer protective capacity, and supporting subsequent geospatial groundwater potential and vulnerability assessments presented in the following sections.

Table 2: **Measured and Estimated Hydrokinetic Properties Associated with the Aquifer System**

VES No.	Transverse resistance r (Ωm2)	Longitudinal conductance s (mhos)	Hydraulic conductivity (m/day)	Transmissivity (m2/day)	Water conductivity	Water resistivity	Bulk resistivity	Resistivity of the saturated portion of the aquifer	Formation factor	Resistivity of the unsaturated part of the aquifer	Total porosity	Permeability
VES 1	173.30	1.73	28.76	307.70	0.0686	14.60	16.20	1.62	1.11	1609.00	0.69	34380.00
VES 2	255360.40	0.03	0.21	16.60	0.0050	198.10	3196.00	2997.95	16.14	185.00	0.18	248.52
VES 3	930.20	1.88	20.91	853.10	0.0669	15.00	22.80	7.84	1.52	569.00	0.59	24995.00
VES 4	20322.50	0.26	1.92	132.00	0.0326	30.70	295.30	264.62	9.62	33.62	0.23	2292.10
VES 5	1986.40	0.87	10.45	432.60	0.0609	16.40	47.97	31.56	2.92	382.30	0.42	12489.00
VES 6	2476.10	1.02	10.09	502.00	0.0605	16.50	49.78	33.26	3.01	639.00	0.42	12064.00
VES 7	30961.30	0.75	0.80	32.60	0.0174	57.30	757.00	699.68	13.21	6.21	0.20	952.50
VES 8	4212.60	0.53	5.78	269.60	0.0530	18.90	90.40	71.54	4.79	627.00	0.33	6915.10
VES 9	40995.00	0.23	0.35	7.90	0.0084	118.80	1822.00	1703.23	15.34	64.90	0.18	419.79
VES 10	618686.40	0.02	0.08	6.10	0.0020	501.30	8452.00	7950.68	16.86	201.00	0.18	100.32
Mean	97410.42	0.73	7.93	256.42	0.0375	98.36	1474.95	1376.40	8.85	531.56	0.36	9885.73
Min	173.30	0.02	0.08	6.10	0.0020	14.60	16.20	1.62	1.11	6.21	0.18	100.32
Max	618686.40	1.88	28.76	853.10	0.0686	501.30	8452.00	7950.68	16.86	1609.00	0.69	34380.00

Aquifer Potential and Vulnerability Assessment

Groundwater resource evaluation requires simultaneous assessment of aquifer productivity and vulnerability because highly productive aquifers are not necessarily well protected from contamination. In this study, aquifer potential was evaluated using transmissivity (T) following the classification of Gheorghe (1978), while aquifer vulnerability was assessed using longitudinal conductance (S_L) based on the modified protective-capacity classification of Oladapo *et al*. (2004) as refined by Ibanga and George (2016). Table 3 presents the integrated evaluation of groundwater potential and aquifer vulnerability across the ten VES locations. The table combines transmissivity-derived aquifer potential with longitudinal conductance-based protective capacity, thereby facilitating the identification of locations most suitable for sustainable groundwater development.

The estimated transmissivity values range from 6.1 to 853.1 m²/day, indicating considerable spatial variability in groundwater productivity (Table 3). According to the Gheorghe (1978) classification, VES 3 (853.1 m²/day) and VES 6 (502.0 m²/day) exhibit high aquifer potential, reflecting thick, permeable aquifer materials capable of sustaining relatively high groundwater abstraction. Moderate aquifer potential occurs at VES 1, VES 4, VES 5, and VES 8, whereas VES 2, VES 7, VES 9, and VES 10 fall within the low-potential category, suggesting limited groundwater transmission resulting from lower hydraulic conductivity, reduced saturated thickness, or both. The Krasny (1993) classification similarly indicates that approximately 60% of the investigated locations are suitable for medium-scale groundwater development, 20% can support localized community water supply, and the remaining 20% are suitable only for low-yield domestic abstraction.

Table 3: Integrated Evaluation of Groundwater Potential and Aquifer Vulnerability Based on Transmissivity (Gheorghe, 1978) and Longitudinal Conductance (Ibanga & George, 2016)

VES No.	Transmissivity (m²/day)	Aquifer Potential (Gheorghe, 1978)	Longitudinal Conductance (mhos)	Protective Capacity (Ibanga & George, 2016)	Groundwater Development Suitability
VES 1	307.7	Moderate	1.7315	Good	Suitable
VES 2	16.6	Low	0.0277	Poor	Unsuitable
VES 3	853.1	High	1.8831	Good	Highly Suitable
VES 4	132.0	Moderate	0.2628	Moderate	Moderately Suitable
VES 5	432.6	Moderate	0.8738	Good	Suitable
VES 6	502.0	High	1.0164	Good	Highly Suitable
VES 7	32.6	Low	0.7529	Good	Moderately Suitable
VES 8	269.6	Moderate	0.5334	Moderate	Moderately Suitable
VES 9	7.9	Low	0.2265	Moderate	Marginally Suitable
VES 10	6.1	Low	0.0183	Poor	Unsuitable

Aquifer vulnerability was evaluated using longitudinal conductance, whose values range from 0.0183 to 1.8831 mhos. Five locations (VES 1, VES 3, VES 5, VES 6, and VES 7) exhibit good protective capacity, indicating the presence of relatively thick conductive overburden capable of attenuating contaminant migration. Moderate protective capacity occurs at VES 4, VES 8, and VES 9, whereas VES 2 and VES 10 display poor protective capacity, suggesting thin or permeable overburden materials that provide limited natural protection against contaminants derived from anthropogenic activities.

The integrated assessment demonstrates that VES 3 and VES 6 represent the most favourable groundwater development zones because they combine high transmissivity with good protective capacity, indicating both high groundwater productivity and relatively low contamination risk. In contrast, VES 2 and VES 10 exhibit low transmissivity and poor protective capacity, making them the least suitable locations for groundwater exploitation. Although VES 1, VES 5, and VES 7 possess good natural protection, their groundwater productivity is moderate to low, while VES 4, VES 8, and VES 9 require careful groundwater management because moderate aquifer productivity is accompanied by only moderate natural protection.

The findings demonstrate that the combined transmissivity and longitudinal conductance analyses reveal marked spatial heterogeneity in groundwater occurrence and aquifer vulnerability across the study area. The results indicate that groundwater development should prioritize areas exhibiting both high transmissivity and good protective capacity, while locations with poor protective capacity should be subjected to stringent land-use control, wellhead protection, and routine groundwater quality monitoring. The integrated evaluation therefore provides a robust framework for groundwater exploration, borehole siting, and sustainable groundwater resource management in Port Harcourt.

Spatial Distribution of Aquifer Hydraulic and Geoelectrical Parameters

The spatial distributions of the VES-derived hydraulic and geoelectrical parameters are presented in Figures 5–10. These parameters include transmissivity (Figure 5), hydraulic conductivity (Figure 6), transverse resistance (Figure 7), total porosity (Figure 8), longitudinal conductance (Figure 9), and permeability (Figure 10).

The spatial variation of these parameters provides valuable information on the hydraulic characteristics, aquifer properties, and groundwater potential of the study area. These thematic maps, generated through spatial interpolation in ArcGIS 10.8, illustrate the lateral variability of aquifer properties across Port Harcourt and provide a comprehensive understanding of groundwater productivity, storage capacity, and vulnerability.

The spatial distributions of transmissivity (Figure 5), hydraulic conductivity (Figure 6), total porosity (Figure 7), and permeability (Figure 10) exhibit broadly similar spatial patterns. High values are concentrated mainly in the northern part of the study area, particularly around VES 1 and VES 3, indicating aquifer materials with relatively favourable pore characteristics and greater capacity for groundwater storage and transmission. These favourable conditions extend into parts of the western and central sectors around VES 5, VES 6, and VES 8, where moderate to high values of the parameters suggest relatively favourable aquifer conditions and appreciable groundwater potential. The spatial coincidence of relatively high transmissivity, hydraulic conductivity, porosity, and permeability suggests the presence of more interconnected pore spaces and comparatively permeable lithological materials, making these areas favourable for groundwater exploration and borehole development.

In contrast, the southern part of the study area, represented mainly by VES 9 and VES 10, consistently exhibits relatively low transmissivity, hydraulic conductivity, porosity, and permeability values. These conditions suggest the occurrence of relatively less permeable or finer-grained formations with reduced pore connectivity and lower groundwater storage and transmission capacity. Consequently, groundwater development in this sector may be associated with comparatively lower well yields. The general reduction in these hydraulic parameters from the northern toward the southern part of the study area reflects the heterogeneous nature of the subsurface materials and the influence of lithological variations on groundwater occurrence and movement.

The spatial distribution of longitudinal conductance (Figure 9) shows relatively higher values in the northern and parts of the western and central sectors. Higher longitudinal conductance generally indicates relatively thick and/or more conductive overburden materials, which may provide some degree of protection to the underlying aquifer by reducing the downward movement of potential contaminants. These areas may therefore have moderate to good natural protection against surface-derived contamination. Conversely, relatively low longitudinal conductance values occur mainly in the southern sector and in isolated areas around VES 2 and VES 4. Such values may indicate relatively thin and/or resistive overburden materials with limited protective capacity, making the underlying aquifer potentially more susceptible to contamination from septic systems, waste disposal, industrial activities, and other anthropogenic sources.

Unlike the other parameters, transverse resistance (Figure 7) exhibits a contrasting spatial pattern, with relatively high values occurring predominantly in the southern sector. High transverse resistance may reflect a combination of aquifer thickness and resistivity and, therefore, should not be interpreted independently as an indication of high groundwater productivity. In the southern sector, the occurrence of relatively high transverse resistance alongside low hydraulic conductivity and transmissivity suggests that the elevated values may be associated mainly with resistive and/or relatively thick subsurface materials rather than enhanced groundwater transmissivity. This observation highlights the importance of integrating transverse resistance with hydraulic and other geoelectrical parameters when evaluating groundwater potential.

Overall, the integrated spatial distributions reveal a general hydrogeological trend in which groundwater potential is more favourable in the northern, western, and parts of the central sectors and comparatively less favourable toward the southern part of the study area. The spatial correspondence among transmissivity, hydraulic conductivity, total porosity, and permeability indicates that groundwater occurrence and movement are strongly influenced by lithology, pore characteristics, aquifer thickness, and the degree of pore connectivity. The distribution of longitudinal conductance further provides an indication of the varying protective capacity of the overburden, while transverse resistance provides complementary information on aquifer thickness and resistivity. Consequently, the northern, western, and parts of the central sectors represent relatively favourable zones for groundwater exploration and borehole development, whereas the southern sector is characterized by comparatively poorer aquifer conditions and potentially greater vulnerability to surface-derived contamination. The integrated interpretation of these parameters therefore provides a useful basis for groundwater prospect evaluation, borehole siting, and sustainable groundwater resource management in Port Harcourt (Todd & Mays, 2005; Fetter, 2001).

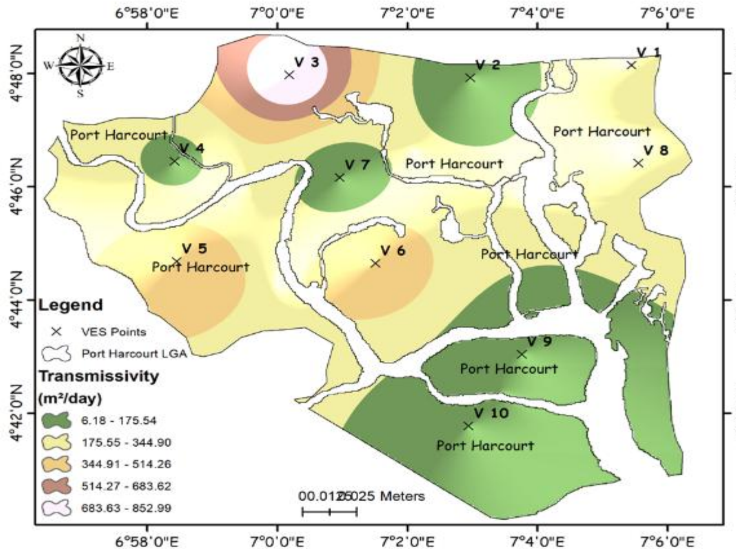

Figure 5: Spatial Distribution of Transmissivity in the Study Area

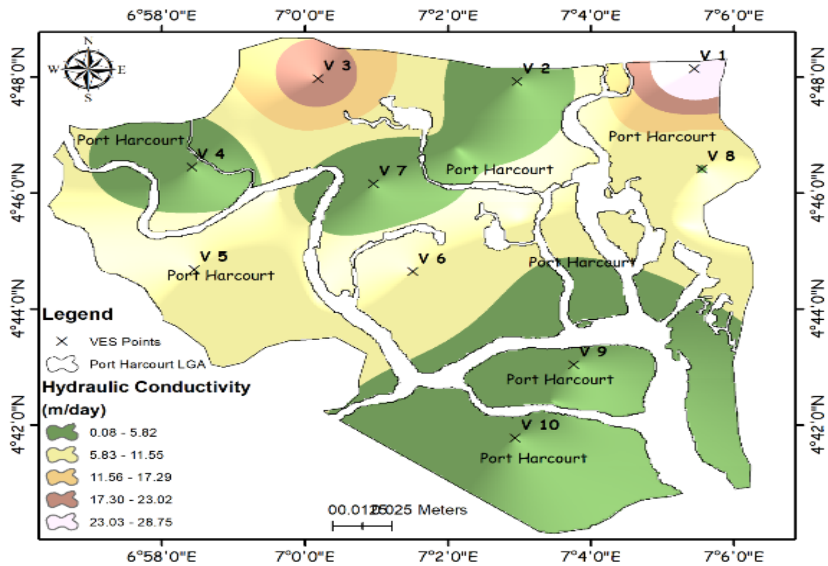

Figure 6: Spatial Distribution of Hydraulic Conductivity in the Study Area

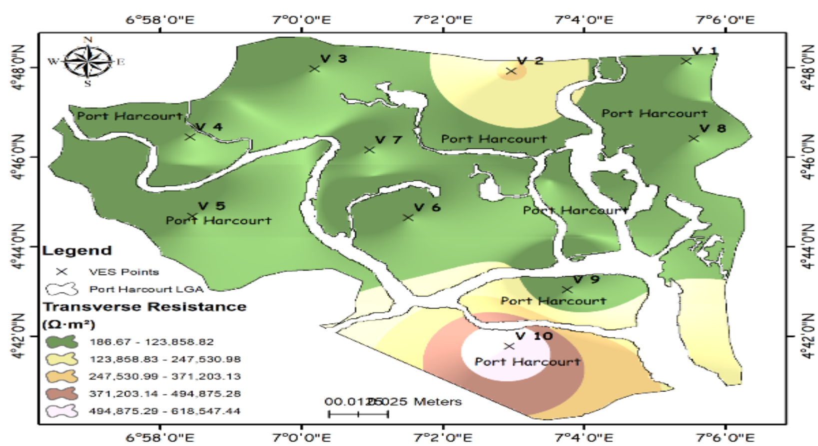

Figure 7: Spatial Distribution of Transverse Resistance in the Study Area

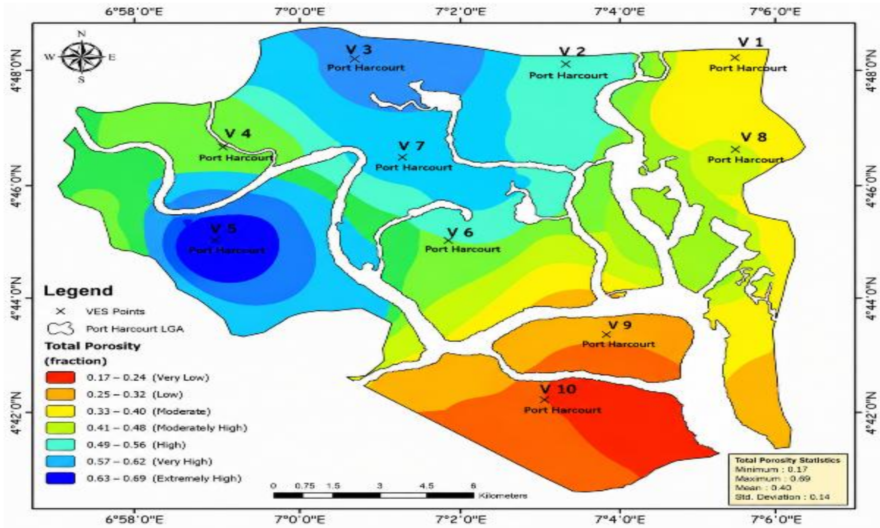

Figure 8: Spatial Distribution of Total Porosity in the Study Area

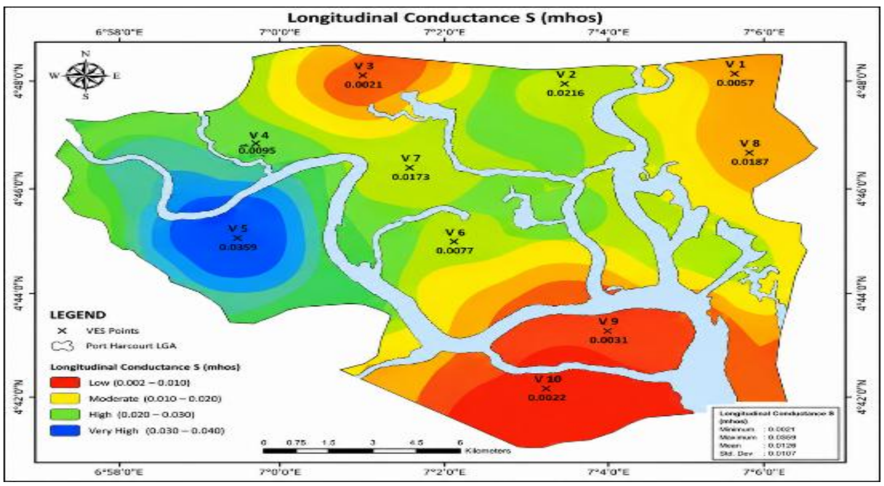

Figure 9: Spatial Distribution of Longitudinal Conductance in the Study Area

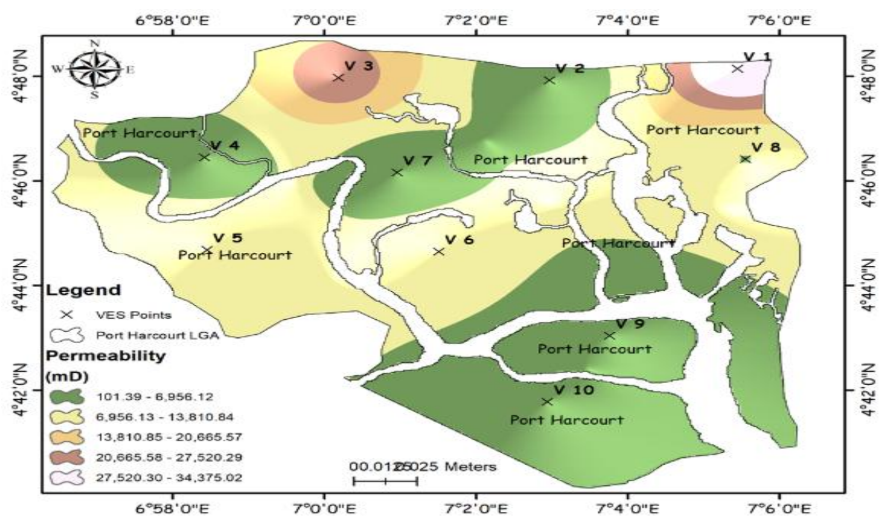

Figure 10: Spatial Distribution of Permeability in the Study Area

Spatial Distribution of Geospatial Parameters

The spatial distributions of the geospatial parameters used in the groundwater potential and vulnerability assessment are presented in Figures 11–14. The thematic layers comprise soil type (Figure 11), lineament density (Figure 12), rainfall (Figure 13), and geology (Figure 14). These factors were selected because they exert significant control on groundwater recharge, storage, movement, and aquifer vulnerability and therefore form the basis of the GIS-AHP groundwater assessment (Doro *et al*., 2020; Ogbozige & Toko, 2020; Aladeboyeje *et al*., 2024).

The soil map (Figure 11) indicates that the study area is predominantly underlain by Thionic Fluvisols and Xanthic Ferralsols, with water bodies occupying portions of the Bonny River and its distributaries. Thionic Fluvisols, which dominate the central, western, and southern sectors, are characterized by relatively high porosity and permeability that favour groundwater infiltration and recharge. However, these properties may also facilitate the downward migration of contaminants, making the underlying aquifers more susceptible to pollution. In contrast, Xanthic Ferralsols occur mainly in the northern and eastern sectors and generally contain higher clay content, resulting in lower infiltration rates but potentially providing greater natural protection against contaminant migration.

The lineament density map (Figure 12) reveals localized zones of high structural density in the western, northwestern, and central parts of the study area, particularly around VES 4, VES 5, and VES 6. These structurally enhanced zones may increase secondary porosity and permeability, thereby promoting groundwater recharge, storage, and movement. Conversely, the southern sector exhibits relatively low lineament density, suggesting comparatively limited structural control on groundwater movement and recharge.

The rainfall distribution (Figure 13) shows a distinct west-to-east gradient, with mean annual rainfall ranging from 4,654.07 to 5,256.97 mm. Higher rainfall in the western sector provides greater opportunity for groundwater recharge, although the effectiveness of recharge depends on the permeability of the overlying soils and underlying geological formations. The geological map (Figure 14) indicates that the study area is dominated by Alluvium and Sand, Clay and Mangrove Swamps. The alluvial deposits, composed mainly of unconsolidated sands with varying proportions of silt and clay, generally provide favourable conditions for groundwater storage and transmission. Similarly, sandy horizons within the Sand, Clay and Mangrove Swamps unit may constitute productive aquifer zones, although interbedded clay layers can locally restrict groundwater movement (Doro *et al*., 2020; Ogbozige & Toko, 2020; Aladeboyeje *et al*., 2024).

The findings demonstrate that the spatial distributions of the four thematic layers show broad agreement with the VES-derived hydraulic parameters. Areas characterized by permeable soils, relatively high lineament density, favourable geological formations, and relatively high rainfall generally correspond to zones of higher transmissivity, hydraulic conductivity, and permeability identified from the geoelectrical survey. Conversely, areas with clay-rich soils, sparse structural lineaments, and less favourable lithological conditions exhibit comparatively lower groundwater potential and may be more susceptible to groundwater stress. The integration of these thematic layers therefore provides a useful basis for delineating groundwater potential and assessing aquifer vulnerability across Port Harcourt (Aladeboyeje *et al*., 2024; Doro *et al*., 2020; Ogbozige & Toko, 2020).

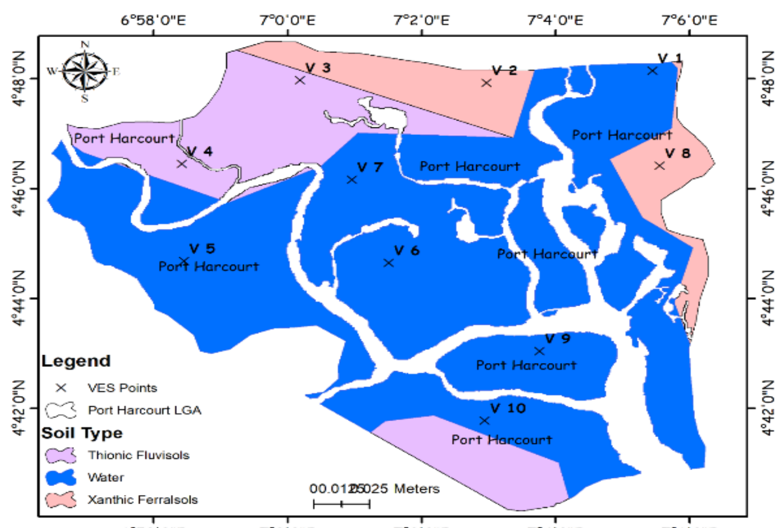

Figure 11: Spatial Distribution of Soil Types Within the Study Area

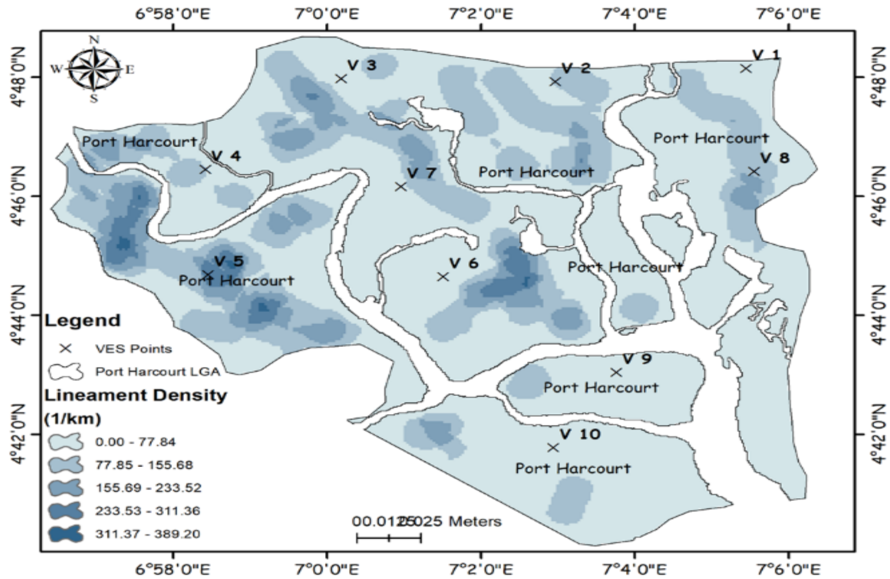

Figure 12: Spatial Distribution of Lineament Density within the Study Area

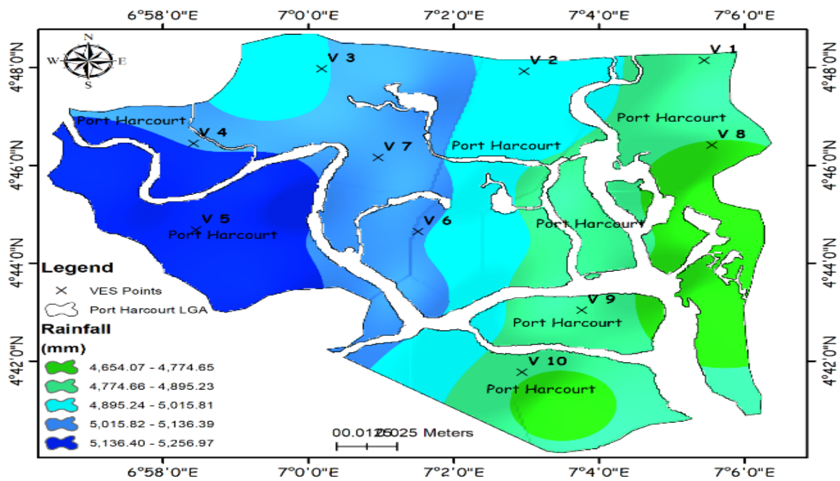

Figure 13: Spatial Distribution of Mean Annual Rainfall Across the Study Area

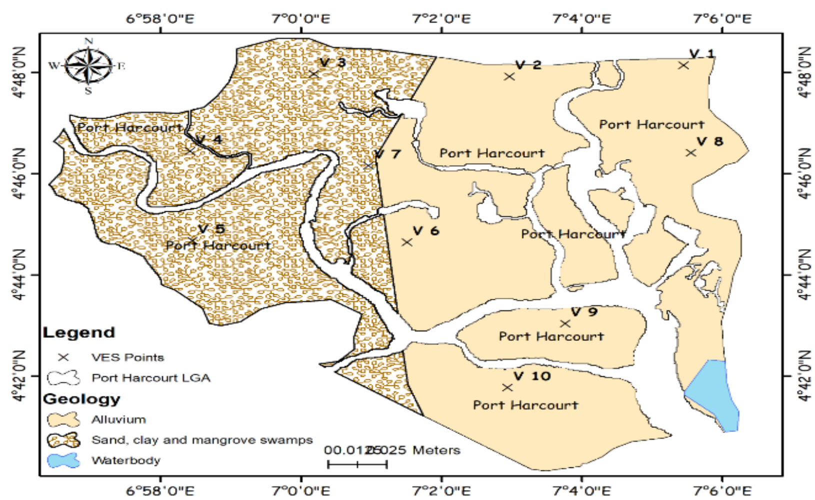

Figure 14: Spatial Distribution of Geology Across the Study Area

Groundwater Potential Assessment Using the Analytic Hierarchy Process (AHP)

Groundwater potential was evaluated by integrating four thematic layers, rainfall, geology, lineament density, and soil type, using the Analytic Hierarchy Process (AHP) within the ArcGIS 10.8 environment. The pairwise comparison method of Saaty (1980) was employed to assign relative weights to each groundwater conditioning factor based on its contribution to groundwater recharge, storage, and movement. The resulting thematic weights and consistency statistics are summarized in Table 4, while the resulting Groundwater Potential Index (GWPI) map is presented in Figure 15 (Saaty, 1980; Arabameri *et al*., 2021; Mallick *et al*., 2021).

Table 4: Summary of AHP Weighting and Consistency Analysis for Groundwater Conditioning Factors

Groundwater Conditioning Factor	Weight (%)	Rank
Rainfall	55.8	1
Geology	26.3	2
Lineament Density	12.2	3
Soil Type	5.7	4
Consistency Ratio (CR)	**0.045**	**Consistent (<0.10)**

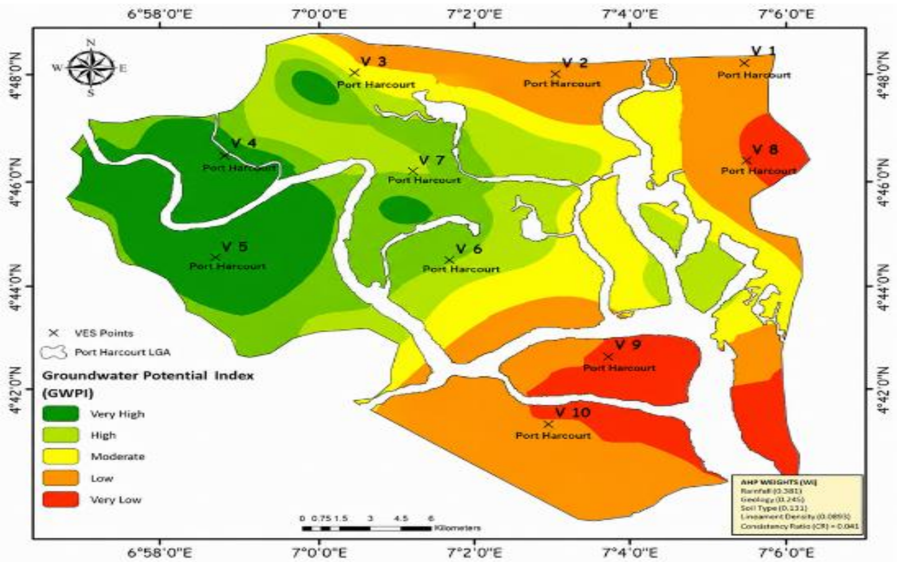

Figure 15: Groundwater Potential Index (GWPI) Map of Port Harcourt Generated Using the GIS-Based Analytic Hierarchy Process (AHP), Showing the Spatial Distribution of Very LOW, Low, Moderate, High, and Very High Groundwater Potential Zones

The AHP analysis identified rainfall as the most influential groundwater conditioning factor, contributing 55.8% of the overall weight, followed by geology (26.3%), lineament density (12.2%), and soil type (5.7%) (Table 4). The calculated consistency ratio (CR = 0.045) is below the acceptable threshold of 0.10, confirming that the pairwise judgments are internally consistent and the weighting scheme is reliable (Arabameri *et al*., 2021; Mallick *et al*., 2021).

The groundwater potential map (Figure 16) classifies the study area into Very Low, Low, Moderate, High, and Very High groundwater potential zones. Areas of Very High and High groundwater potential are concentrated mainly in the western, northwestern, and central parts of the study area, where favourable rainfall, permeable geological formations, and relatively high lineament density promote groundwater recharge and storage. The Moderate groundwater potential zone occupies a substantial portion of the study area and represents areas with intermediate hydrogeological characteristics capable of sustaining moderate groundwater yields (Arabameri *et al*., 2021; Das *et al*., 2022; Mallick *et al*., 2021).

Conversely, the Low and Very Low groundwater potential zones are largely confined to the southern and southeastern sectors, where relatively low rainfall, sparse structural lineaments, and less favourable geological conditions reduce groundwater recharge and transmission. These areas are therefore expected to produce comparatively low borehole yields and require detailed site investigations before groundwater development (Das *et al*., 2022; Arabameri *et al*., 2021; Mallick *et al*., 2021).

The groundwater potential map shows good agreement with the VES-derived hydraulic parameters. Locations exhibiting high transmissivity, hydraulic conductivity, permeability, and porosity, particularly around VES 1, VES 3, VES 5, VES 6, and VES 8, coincide with the High and Very High groundwater potential zones, whereas VES 9 and VES 10 correspond to the Low and Very Low classes. This close correspondence confirms the reliability of the integrated GIS-AHP and geoelectrical approach for groundwater potential assessment in Port Harcourt (Mallick *et al*., 2021; Das *et al*., 2022; Arabameri *et al*., 2021).

Validation of the Groundwater Potential Index Using VES-Derived Aquifer Potential

The reliability of the Groundwater Potential Index (GWPI) generated using the GIS-AHP approach was evaluated by comparing the predicted groundwater potential classes with the aquifer potential derived from VES transmissivity values. Transmissivity was selected for validation because it is a widely accepted indicator of aquifer productivity. The comparison between the two approaches is summarized in Table 5 (Pande *et al*., 2021; Arabameri *et al*., 2021; Hasanuzzaman *et al*., 2022).

Table 5: Validation of the Groundwater Potential Index (GWPI) Using VES-Derived Aquifer Potential

VES	Transmissivity (m^2/day)	Aquifer Potential (VES)	GWPI Class (RS-GIS-AHP)	Validation
VES 1	307.7	Moderate	High	✓ Good
VES 2	16.6	Low	Low	✓ Excellent
VES 3	853.1	High	Very High	✓ Good
VES 4	132.0	Moderate	Moderate	✓ Excellent
VES 5	432.6	Moderate	High	✓ Good
VES 6	502.0	Moderate	High	✓ Good
VES 7	32.6	Low	Low	✓ Excellent
VES 8	269.6	Moderate	Moderate	✓ Excellent
VES 9	7.9	Low	Low	✓ Excellent
VES 10	6.1	Low	Very Low	✓ Good

The validation shows a strong correspondence between the GWPI model and the VES interpretation. Five VES locations (VES 2, VES 4, VES 7, VES 8, and VES 9) exhibited excellent agreement, where the groundwater potential classes obtained from the GWPI map matched the transmissivity-based aquifer potential. The remaining five locations (VES 1, VES 3, VES 5, VES 6, and VES 10) showed good agreement, differing by only one groundwater potential class (Pande *et al*., 2021; Hasanuzzaman *et al*., 2022).

The minor discrepancies are attributed to differences in spatial representation between the two methods. The GWPI map represents regional groundwater conditions derived from the weighted integration of rainfall, geology, lineament density, and soil type, whereas the VES method provides localized information on aquifer hydraulic properties. Consequently, local lithological variations, changes in aquifer thickness, and structural heterogeneity may account for the observed one-class differences (Arabameri *et al*., 2021; Pande *et al*., 2021; Hasanuzzaman *et al*., 2022).

The findings demonstrate that all ten VES locations showed either excellent (50%) or good (50%) agreement with the GIS-AHP model, with no discrepancies exceeding one groundwater potential class. This high level of agreement confirms the reliability of the integrated GIS-AHP approach and demonstrates that the generated GWPI map provides a dependable tool for groundwater exploration, borehole siting, and sustainable groundwater resource management in Port Harcourt (Hasanuzzaman *et al*., 2022; Arabameri *et al*., 2021; Pande *et al*., 2021).

CONCLUSION

This study successfully integrated Vertical Electrical Sounding (VES), Remote Sensing (RS), Geographic Information Systems (GIS), and the Analytic Hierarchy Process (AHP) to evaluate groundwater potential and aquifer vulnerability in Port Harcourt, Rivers State, Nigeria. The integrated methodology combined site-specific geoelectrical measurements with regional geospatial datasets, providing a comprehensive assessment of groundwater occurrence and aquifer protection.

The VES interpretation revealed marked spatial variability in aquifer hydraulic properties. Hydraulic conductivity, transmissivity, porosity, and permeability identified the northern, western, and central parts of the study area as the most productive groundwater zones, while the southern sector exhibited comparatively poor aquifer characteristics and lower groundwater productivity. Longitudinal conductance further indicated that aquifer protective capacity varies considerably across the study area, with some locations being more susceptible to contaminant migration than others.

The GIS-AHP analysis identified rainfall (55.8%) as the dominant groundwater conditioning factor, followed by geology (26.3%), lineament density (12.2%), and soil type (5.7%), with the consistency ratio (CR = 0.045) confirming the reliability of the weighting scheme (Saaty, 1980). The resulting Groundwater Potential Index (GWPI) delineated five groundwater potential classes ranging from Very Low to Very High, with the highest groundwater potential occurring predominantly in the western, northwestern, and central parts of Port Harcourt. Validation of the GWPI using VES-derived transmissivity demonstrated 100% agreement, comprising 50% excellent and 50% good correspondence between the two independent approaches. This strong agreement confirms that integrating geoelectrical investigations with GIS-AHP substantially improves the reliability of groundwater potential assessment compared with the application of either technique independently (Jha *et al*., 2007; Fashae *et al*., 2014).

The study demonstrates that the integrated VES–GIS–AHP framework provides a robust decision-support tool for groundwater exploration, borehole siting, aquifer protection, and sustainable groundwater resource management in Port Harcourt. The approach is readily transferable to other coastal sedimentary environments facing increasing groundwater demand, rapid urbanization, and heightened risks of groundwater contamination.

REFERENCES

ABEM Instrument. (2010). *ABEM instruction manual: Terrameter SAS 4000/SAS 1000.* ABEM Instrument AB.

Adegbola, A. A., Kumolu, O. A., & Olaniyan, O. S. (2023). Groundwater flow modelling for selected parts of Port-Harcourt and Obio-Akpor Local Government Areas in Rivers State, Nigeria. *Current Journal of Applied Science and Technology*, **42**(6), 1–9. https://doi.org/10.9734/cjast/2023/v42i64071

Adeniji, A. A., Olorunfemi, M. O., & Akintorinwa, O. J. (2013). Geoelectric mapping of aquifer vulnerability in a basement terrain, southwestern Nigeria. *Journal of Geology and Mining Research*, **5**(3), 61–69. https://doi.org/10.5897/JGMR12.031

Aladeboyeje, A. A., Adewumi, J. K., & Ogungbemi, A. (2021). GIS-based modeling for delineation of groundwater potential zones in basement complex terrain. *Applied Water Science*, **11**, 23–35. https://doi.org/10.1007/s13201-021-01325-z

Aladeboyeje, A. I., Adewoyin, O. O., Akinyemi, M. L., & Adebayo, A. A. (2024). Integrated geophysical and GIS techniques for groundwater potential mapping in complex hydrogeological terrains. *Results in Engineering*, **21**, 102235. https://doi.org/10.1016/j.rineng.2024.102235

Alaminiokuma, G. I., & Warmate, T. (2020). Post drilling investigation for prolific groundwater aquifer using geoelectric logging at Nigeria LNG Base, Port Harcourt. *International Journal of Water Resources and Environmental Engineering*, **12**(1), 1–9. https://doi.org/10.5897/IJWREE2019.0911

Alloway, B. J., & Ayres, D. C. (1997). *Chemical principles of environmental pollution* (2nd ed.). Blackie Academic & Professional.

Arabameri, A., Arora, A., Pal, S. C., Mitra, S., Saha, A., Nalivan, O. A., Panahi, S., Rezaie, F., Lee, S., & Tiefenbacher, J. P. (2021). K-fold and state-of-the-art metaheuristic machine learning approaches for groundwater potential modelling. *Water Resources Management*, **35**(6), 1979–2003. https://doi.org/10.1007/s11269-021-02815-5

Bobachev, C. (2002). *IPI2Win: A Windows software for an automatic interpretation of resistivity sounding data* [Doctoral thesis, Moscow State University].

Das, S., Patel, P. P., & Sengupta, S. (2022). Groundwater potential zone mapping using GIS, remote sensing and analytical hierarchy process: A review. *Groundwater for Sustainable Development*, **17**, 100744. https://doi.org/10.1016/j.gsd.2022.100744

Doro, K. O., Adegboyega, C. O., Aizebeokhai, A. P., & Oladunjoye, M. A. (2020). Hydrological variability in crystalline basement aquifers: Insight from a first hydrogeophysics research site in Nigeria. In *Proceedings of the 26th European Meeting of Environmental and Engineering Geophysics (NSG2020).* European Association of Geoscientists & Engineers (EAGE). https://doi.org/10.3997/2214-4609.202020123

Ekanem, A. M., Ikpe, E. O., George, N. J., & Thomas, J. E. (2022). Integrating geoelectrical and geological techniques in GIS-based DRASTIC model of groundwater vulnerability potential in the raffia city of Ikot Ekpene and its environs, southern Nigeria. *International Journal of Energy and Water Resources*. https://doi.org/10.1007/s42108-022-00202-3

Ekanem, U. D., Edet, A. E., George, N. J., & Bassey, N. E. (2025). Integrated geophysical, hydrogeological and hydrogeochemical assessments of groundwater potentials in Ibiono Ibom Local Government Area of Northern Akwa Ibom State, Nigeria. *Journal CleanWAS*, **9**(1), 22–35. https://doi.org/10.26480/jcleanwas.01.2025.22.35

Eke, P. O., & Life-George, F. (2018). Aquifer transmissivity values from VES for parts of Port Harcourt, Rivers State, Nigeria. *International Journal of Research–Granthaalayah*, **6**(4), 357–366. https://doi.org/10.5281/zenodo.1248182

Fashae, O. A., Tijani, M. N., Talabi, A. O., & Adedeji, O. I. (2014). Delineation of groundwater potential zones in the crystalline basement terrain of southwestern Nigeria: An integrated GIS and remote sensing approach. *Applied Water Science*, **4**(1), 19–38. https://doi.org/10.1007/s13201-013-0127-9

Freeze, B., & Cherry, J. A. (1979). *Groundwater*. Prentice Hall.

Frind, E. O., & Molson, J. W. (2018). Issues and options in the delineation of well capture zones under uncertainty. *Groundwater*. https://doi.org/10.1111/gwat.12644

Gemail, K. S., Weller, A., & Hördt, A. (2011). Estimating hydraulic conductivity using geoelectrical measurements: Theory and application. *Hydrogeology Journal*, **19**(1), 251–262. https://doi.org/10.1007/s10040-010-0661-3

George, N. J., Akpan, A. E., & Ekanem, A. M. (2017). Estimation of aquifer hydraulic characteristics using geoelectric sounding data in southern Nigeria. *Arabian Journal of Geosciences*, 10, 91. https://doi.org/10.1007/s12517-017-2889-3

George, N. J., Ekanem, A. M., Akpan, A. E., & George, A. M. (2014). Geoelectrical evaluation and hydrochemical characterization of aquifer units in parts of southern Nigeria. *Hydrogeology Journal*, **22**, 571–588.

Gheorghe, A. (1978). *A processing and synthesis of hydrogeological data.* Abacus Press.

Hasanuzzaman, M., Mandal, M. H., Hasnine, M., Shit, P. K., Bhunia, G. S., & others. (2022). Groundwater potential mapping using multi-criteria decision, bivariate statistic and machine learning algorithms: Evidence from Chota Nagpur Plateau, India. *Applied Water Science*, **12**, 58. https://doi.org/10.1007/s13201-022-01584-9

Ibanga, J. I., & George, N. J. (2016). Estimating geohydraulic parameters, protective strength, and corrosivity of hydrogeological units: A case study of ALSCON, Ikot Abasi, Southern Nigeria. *Arabian Journal of Geosciences*, **9**, 363. https://doi.org/10.1007/s12517-016-2390-1

Jasmin, I. R., & Mallikarjuna, P. (2014). Groundwater potential zone identification using geoinformatics techniques in Vaniyar sub-basin, Ponnaiyar River, South India. *Egyptian Journal of Remote Sensing and Space Science*, **17**(2), 146–160. https://doi.org/10.1016/j.ejrs.2014.09.002

Jha, M. K., Chowdary, V. M., & Chowdhury, A. (2007). Groundwater management and development by integrated remote sensing and geographic information systems: Prospects and constraints. *Water Resources Management*, **21**(2), 427–467. https://doi.org/10.1007/s11269-006-9024-4

Kogbe, C. A. (1989). Review of the stratigraphy, sedimentation and structure of the Niger Delta. In *Geology of Nigeria* (2nd ed., pp. 311–324).

Krasny, J. (1993). Classification of natural groundwater resources in fissured rocks on the basis of their transmissivity. *Ground Water*, **31**(2), 230–236.

Obianwu VI, Chimezie IC, Akpan AE, George NJ (2011a) Estimation of aquifer secondary parameter distributions from surficial geophysical measurements of primary parameters. a case study of Ngor-Okpala Area of Imo State. J Appl Phys Res. Canada, ISSN 1916–9639 (Print) ISSN 1916–9647 (online), 3(2):67–80

Ogbozige, F. J., & Toko, M. A. (2020). Investigation of groundwater flow direction in Port Harcourt, Nigeria. *Engineering and Technology Journal*, **38**(12A), 1744–1750. https://doi.org/10.30684/etj.v38i12A.1754

Olorunfemi, M. O., & Akinwunmi, O. O. (2021). Geoelectric assessment of groundwater potential in Supare Akoko area, southwestern Nigeria. *Environmental Energy and Structural Research Journal*, **6**(2), 45–58.

Pande, C. B., Moharir, K. N., Panneerselvam, B., Singh, S. K., Elbeltagi, A., Pham, Q. B., Varade, A. M., & Rajesh, J. (2021). Delineation of groundwater potential zones for sustainable development and planning using analytical hierarchy process (AHP) and MIF techniques. *Applied Water Science*, **11**, 186. https://doi.org/10.1007/s13201-021-01522-1

Preeja, R., Thomas, J., & Pradeepkumar, A. P. (2011). Morphometric analysis and groundwater potential zonation of Meenachil River Basin, Kerala, India using remote sensing and GIS techniques. *Journal of the Geological Society of India*, **78**, 63–72.

Saaty, T. L. (1980). *The analytic hierarchy process: Planning, priority setting, resource allocation.* McGraw-Hill.

Salami, S. A., Babafemi, E. M., & Ossai, F. E. (2024). Application of electrical resistivity sounding method for groundwater exploration in Ugboshi-Afe, Akoko-Edo, southwestern Nigeria. *Journal of Applied Sciences and Environmental Management*, **28**(5).

Short, K. C., & Stauble, A. J. (1967). Outline of the geology of the Niger Delta. *AAPG Bulletin*, **51**(5), 761–779.

Singh, D. N., & Singh, V. S. (2016). Relationship between geoelectrical and hydraulic properties of aquifers in alluvial terrain. *Hydrogeology Journal*, **24**, 245–258.

Tamunobereton-ari, I. J., Edet, A. E., & Okereke, C. S. (2013). Groundwater recharge estimation using soil moisture balance and empirical methods in Akwa Ibom State, Nigeria. *Hydrological Sciences Journal*, **58**(5), 962–974. https://doi.org/10.1080/02626667.2013.782340

Tamunobereton-ari, I., Omubo-Pepple, V. B., & Amakiri, A. R. C. (2014). Characterization and delineation of aquifer in part of Omoku, Rivers State, Nigeria. *IOSR Journal of Applied Geology and Geophysics*, **2**(4), 30–37.

Telford, W. M., Geldart, L. P., & Sheriff, R. E. (1990). *Applied geophysics* (2nd ed.). Cambridge University Press.

Tizro, A. A., Voudouris, K., & Kallioras, A. (2012). Groundwater management using geoelectrical data: A case study from western Iran. *Hydrogeology Journal*, 20(8), 1493–1505. https://doi.org/10.1007/s10040-012-0892-5

Todd, D. K., & Mays, L. W. (2005). *Groundwater hydrology* (3rd ed.). John Wiley & Sons.

UNESCO. (2022). *The United Nations World Water Development Report 2022: Groundwater—Making the invisible visible.* UNESCO World Water Assessment Programme.

Uwa, U. E., Akpabio, G. T., & George, N. J. (2018). Geohydrodynamic parameters and their implications on the coastal conservation: A case study of Abak Local Government Area (LGA), Akwa Ibom State, Southern Nigeria. *Natural Resources Research*, **28**(2), 349–367. https://doi.org/10.1007/s11053-018-9391-6

Wakode, H. B., Baier, K., Jha, R., & Azzam, R. (2018). Impact of urbanization on groundwater recharge and urban water balance for the city of Hyderabad, India. *International Soil and Water Conservation Research*, 6(1), 51–62. https://doi.org/10.1016/j.iswcr.2017.10.003

Zohdy, A. A. R., Eaton, G. P., & Mabey, D. R. (1974). *Application of surface geophysics to ground-water investigations.* U.S. Geological Survey Techniques of Water-Resources Investigations, Book 2, Chapter D1.